Environment and Natural Resources Journal

Volume 24
Issue X
2026

Attenuation of Organic Matter in Landfill Leachate: Seasonal Characterization and Soil Column Evaluation

Lokesh Sapkota[1], Rajendra Joshi[2], Bikash Adhikari[1], Bijay Thapa[3], Sophie Shrees[4], Aalekh Bhattarai[4], and Anish Ghimire[5*]

[1]*Department of Environmental Engineering, School of Engineering, Kathmandu University, Dhulikhel, Nepal*
[2]*Department of Pharmacy, School of Science, Kathmandu University, Dhulikhel, Nepal*
[3]*EnergizeNepal Program, Kathmandu University, Dhulikhel, Nepal*
[4]*Soil, Water and Air Testing Laboratories Pvt Ltd, Bulbule Marga-10, Thapagaun, Kathmandu, Nepal*
[5]*Environmental Engineering and Management, Asian Institute of Technology, Pathum Thani 12120, Thailand*

ARTICLE INFO

Received: 28 Aug 2025
Received in revised: 2 Dec 2025
Accepted: 16 Dec 2025
Published online: 29 Jan 2026
DOI: 10.32526/ennrj/24/20250233

Keywords:
Landfill leachate/ Leachate pollution index/ Fixed-bed column/ Attenuation/ Breakthrough curves/ Model evaluation

*** Corresponding author:**
E-mail: anish-ghimire@ait.asia

ABSTRACT

Landfill leachate (LL) from landfills and open dumpsites poses significant risks to surrounding soils and water bodies. This study investigated seasonal variations in physicochemical and heavy metal characteristics of LL at the newly operational Bancharedada landfill site in Nepal using the Leachate Pollution Index (LPI). It also evaluated the attenuation of organic content, measured as chemical oxygen demand (COD), across different soil textures using fixed-bed column tests. Kinetics analyses employed the Yoon-Nelson model (YNM), Thomas model (TM), and Adam and Bohart model (ABM). The biological oxygen demand (BOD_5)/COD ratio ranged from 0.44 to 0.51, with higher values in the dry seasons and lower values during the monsoon, indicating rainfall-induced dilution of organic pollutants. The bed saturation time for COD removal was longest in clayey soil (35 days) and shortest in sandy soil (4 days). YNM provided the best model fit and was therefore applied for COD breakthrough prediction across soil textures. YNM rate constants (KYN) were lower in clayey soils and higher in sandy soils, thereby increase in breakthrough times (τ) and adsorption capacities (Qo) in clayey soils whereas the sandy soils shows the opposite trend, highlighting the strong influence of soil texture on COD attenuation potential.

HIGHLIGHTS

- Seasonal LL quality was assessed using the Leachate Pollution Index.
- Fixed-bed column tests evaluated COD attenuation in seven soil textures.
- The Yoon-Nelson model best predicted COD removal across soil types.
- Soil texture strongly influenced COD removal.

1. INTRODUCTION

In 2016, global municipal solid waste generation reached 2.01 billion tonnes and is projected to reach 3.40 billion tonnes by 2050. South Asian cities contributed 334 million tonnes in 2016, with estimates rising to 466 million tonnes by 2030 and 661 million tonnes by 2050 (Kaza et al., 2018). In Nepal, urbanisation has substantially increased waste generation (Pathak et al., 2020), amounting to approximately 1.8 million tonnes annually and requiring 35 hectares of land annually for untreated disposal (Goyal et al., 2020). Current disposal practices include open dumping (48.6%), burning (32.1%), and river dumping (27.4%) (Central Bureau of Statistics, 2020), leading to significant environmental challenges such as greenhouse gas emissions, land and water contamination, and climate change.

Kathmandu Metropolitan City generated approximately 766 tonnes/day of waste in 2021, a figure projected to reach 1,259 tonnes/day by 2035 (Khanal, 2023). Waste from the Kathmandu Metropolitan City and nearby municipalities is currently managed at the Bancharedada landfill site, located 27 km northwest of Kathmandu. The

Citation: Sapkota L, Joshi R, Adhikari B, Thapa B, Shrees S, Bhattarai A, Ghimire A. Attenuation of organic matter in landfill leachate: Seasonal characterization and soil column evaluation. Environ. Nat. Resour. J. 2026;24(X):xx-xx.

Bancharedada landfill site still lacks a facility for treating leachate. LL is a byproduct of waste decomposition and varies in composition depending on rainfall, landfill age, and waste characteristics (Nayanthika et al., 2018; Nawaz et al., 2020). The Leachate Pollution Index (LPI) can be used to leachate contamination potential and to compare compliance with the regulatory standards (Hussein et al., 2019).

Leachate treatment mechanisms include biological, chemical, and physicochemical processes such as activated sludge, advanced oxidation, adsorption, and membrane filtration (Teng et al., 2021). In landfill sites, the soil cover used for daily waste covering has varying permeability and can function as an in-situ treatment medium for LL (Yidong et al., 2012). This underscores the need to understand the containment and attenuation behaviour of LL across different soil textures. However, research on leachate-soil interactions and natural attenuation of contaminants remains limited (Gonçalves et al., 2019).

Clayey soil is commonly preferred as a daily landfill cover materials due to its low hydraulic conductivity and high sorption capacity, which enhance pollutant retention (Qi et al., 2013; Chetri and Reddy, 2021). Soil texture, particularly the fine content in clayey soil, plays a key role in pollutant attenuation by attracting ions and enhancing adsorption (Regadío et al., 2015; Cronan, 2018). Column experiments are widely used to simulate field conditions and evaluate leachate-soil interactions over time (Naka et al., 2016). This highlights the significant influence, particularly, remain limited. This highlights the significant influence of soil texture on pollutant attenuation and containment. However, studies investigating the attenuation of organic contaminants across localised soil textures, particularly in the South Asian context, remain limited.

This study is the first to investigate the behaviour of COD as an absorbate across different soil textures found in Nepal, focusing on their attenuation capacity to prevent subsoil contamination. Additionally, the study examined seasonal variations in LL physicochemical and heavy metal composition and applied the LPI to identify the key contributing pollutants. Fixed-bed column experiments were conducted to evaluate COD-soil interactions, and the resulting data were analysed using three kinetic models (YNM, TM, and ABM) to quantify COD removal rates. Model performance was evaluated based on R^2 values, and the best-fitting model was used to predict COD attenuation across soil textures, providing valuable insights to support the design of effective landfill liner materials.

2. METHODOLOGY

2.1 Materials

2.1.1 Leachate and soil sampling

Leachate samples were collected from the Bancharedada landfill site in Nepal, as shown in Figure 1. The site is located 27 km northwest of Kathmandu and 2 km west of the previous Sisdole landfill site, within the boundaries of Kakani Rural Municipality (Ward number 2) in Nuwakot District and Dhunibesi Municipality (Ward number 1) in Dhading District. Leachate sampling was conducted over 12 months, with a total of 12 samples collected from March 2023 to February 2024, covering the dry, summer, wet, and winter seasons. The samples were collected and preserved according to the Standard Methods for the Examination of Water and Wastewater (Baird et al., 2017).

A purposive sampling technique was used for the first three soil samples (S1, S2, and S3), selected based on clay, sand, and silt content exceeding 50%, as per soil maps prepared by the National Soil Science Research Center (NSSRC), a unit under the Nepal Agricultural Research Council (NARC), Government of Nepal (https://soil.narc.gov.np/). Soil samples S4 and S5 were collected from the Sisdole landfill site, while S6 and S7 were taken from the Bancharedada landfill site. All samples were collected manually at a depth of 0-15 cm after clearing surface debris. The details of the soil sampling sites used in the column experiments are shown in Table 1.

2.1.2 Column tests setup and experimental design

Column tests were conducted using leachate samples applied to seven soil types (clayey, silt loam, sandy, loam, sandy loam, clay loam, and silt loam) under controlled conditions. Polyvinyl chloride pipes (4.5 cm diameter, 30 cm packing height) were used, with 2 mm gravel and sand layers placed at the top and bottom to ensure steady flow. Each day, 250 mL of leachate was applied to each column (25 mL every 30 min for 5 h) over one month. Effluents were collected every 12 h for COD analysis. Bulk densities of the soils ranged from 1.33 to 1.65 g/cm^3. The column setup followed the (Organisation for Economic Co-operation and Development (OECD), 2004) and Naka et al. (2016) guidelines. A schematic of the experimental setup is shown in Figure 2.

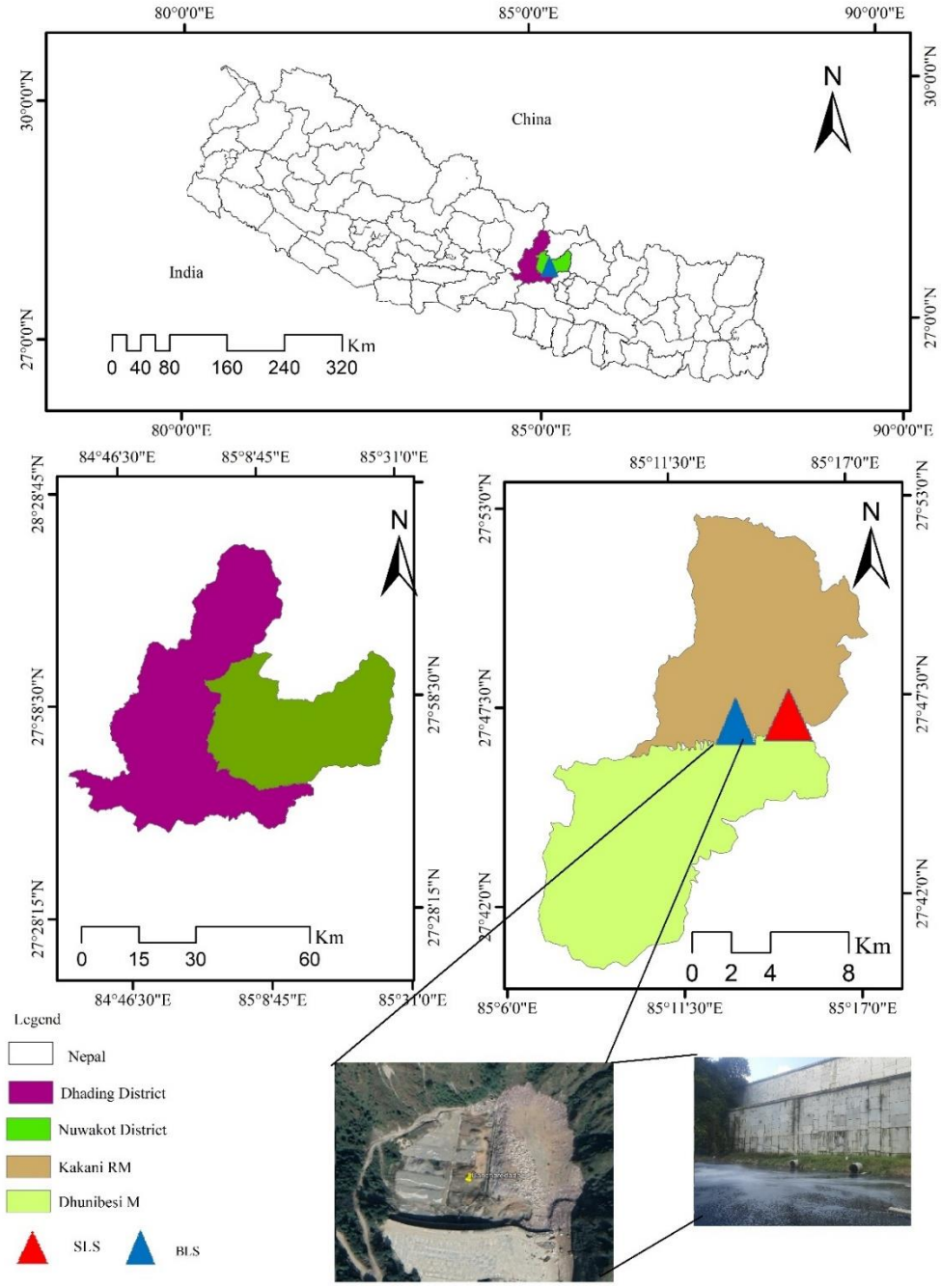

Figure 1. Map of Sisdole landfill site located in Kakani rural municipality (RM), Nuwakot district and Bancharedada landfill site located on the border of Kakani Rural Municipality and Dhunibesi municipality, Dhading district, Bagmati province, Nepal (image from Google Map taken in 2023)

Table 1. Soil sampling sites used in the column experiments

Soil samples	Latitude and longitude	Elevation, above mean sea level (m)	District/RM/Mun	Province
S1 (clayey)	27º39'15.45", 83º02' 10.23"	112	Kapilbastu/ Buddhabhumi Municipality-4	Lumbini
S2 (silt loam)	26º 26' 45", 87º 21' 1"	69	Morang/ Jahada Rural Municipality-6	Koshi
S3 (sandy)	27º45' 48.61", 85º 21' 59.80"	1388	Kathmandu/Budhanilkanta Municipality-12	Bagmati
S4 (loam)	27º46' 36.91", 85º 14' 48.81"	1154	Nuwakot/Kakani Rural Municipality-3	Bagmati

Table 1. Soil sampling sites used in the column experiments (cont.)

Soil samples	Latitude and longitude	Elevation, above mean sea level (m)	District/RM/Mun	Province
S5 (Sandy loam)	27º46'32.56", 85º 14' 37.56"	1130	Nuwakot/Kakani Rural Municipality-3	Bagmati
S6 (clay loam)	27º 46' 25.79", 85º 13' 42.20"	1053	Dhading/ Dhunibesi Municipality-1	Bagmati
S7 (silt loam)	27º 46' 31.35", 85º 13' 47.23"	1062	Dhading/ Dhunibesi Municipality-1	Bagmati

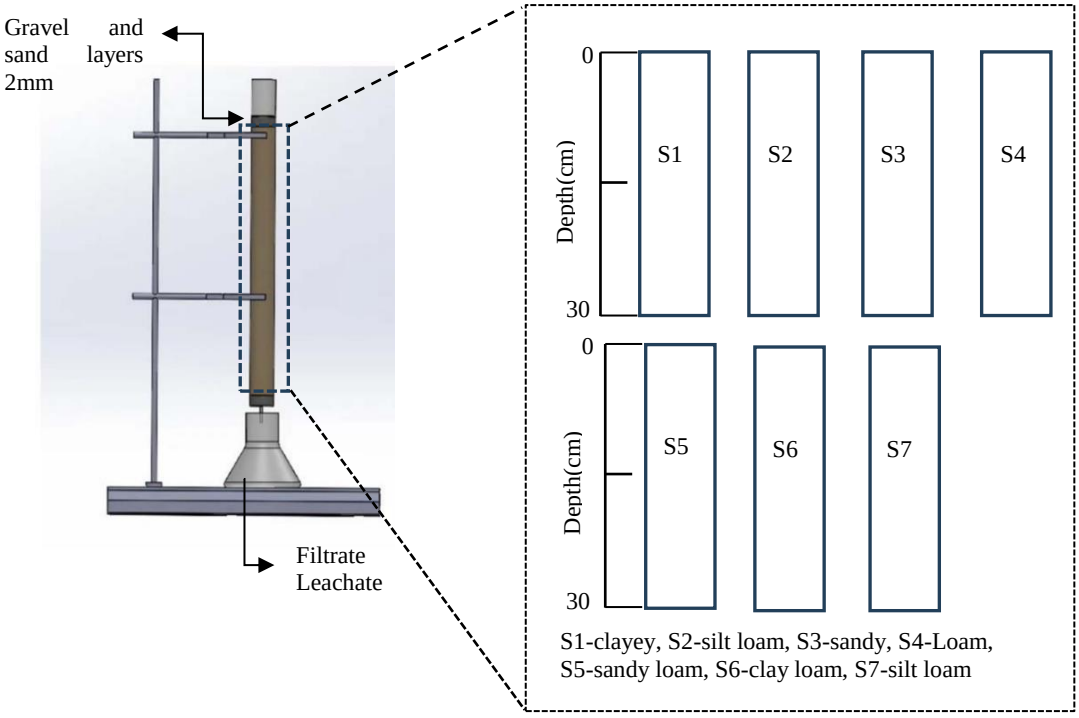

Figure 2. A schematic of the experimental setup of the column test

2.2 Methods

2.2.1 Analytical methods

The analysis of major physical and chemical properties of raw leachate and effluent obtained from the soil column tests (liquid filtrate) was conducted using standard procedures outlined in the Standard Methods for the Examination of Water and Wastewater, APHA 23rd Edition (Baird et al., 2017). Table 2 presents the parameters, methods, instrumentation, and references used for the analysis of leachate and soil samples.

2.2.2 Calculation of the leachate pollution index

LPI measures the contamination potential of LL (Lothe and Sinha, 2017). It incorporates 18 parameters, including COD, BOD_5, TKN, NH_3-N, pH, TDS, Cr, Pb, Hg, As, cyanide, phenolic compounds, Zn, Ni, Cu, Cl, Fe, and total coliform (Kumar and Alappat, 2005). Due to analytical limitations, cyanide and phenolic compounds were not analysed in this study. The overall LPI and three sub-indices – LPI Organic (LPI_{or}), LPI inorganic (LPI_{in}), and LPI heavy metals (LPI_{hm}) – were calculated to assess contamination potential of each component. Each sub-index was estimated using the concentration values of the available leachate parameters using equation (1):

$$LPI = \frac{\sum_{i=n}^{n} W_i P_i}{\sum_{i=1}^{n} W_i} \quad (1)$$

Then, overall LPI was estimated based on equation (2):

$$\text{Overall LPI} = 0.232\, LPI_{or} + 0.257\, LPI_{in} + 0.511\, LPI_{hm} \quad (2)$$

Where; W_i is the weight for the i^{th} pollutant variable, P_i is the sub-index score of the i^{th} pollutant variable, and n is the number of leachate pollutant variables.

Table 2. Analytical methods for leachate and soil samples

Parameter	Method	Instrumentation	Reference
Leachate samples			
pH	Electrode	pH meter	4500-H^+ B. APHA
Conductivity	Electrode	Conductivity meter	2510 B. APHA
Turbidity	Nephelometric	Turbidity meter	2130 B. APHA
Total dissolved solids	Gravimetric	Oven drying at 180°C	2540 C. APHA
BOD_5	Iodometric titration	BOD Incubator	5210 B. APHA
COD	Closed reflux colorimetric	Colorimeter	5220 D. APHA
Ammoniacal Nitrogen (NH_3-N)	Phenate Method	Spectrophotometer	4500- NH_3 F. APHA
Nitrate-Nitrogen (NO_3-N)	Colorimetric	Spectrophotometer	4500-NO_3^-B. APHA
Total Kjeldahl Nitrogen (TKN)	Semi Micro Kjeldahl method	Kjeldahl apparatus	4500-N_{org} C. APHA
Zinc (Zn) Copper (Cu) Manganese (Mn) Chromium (Cr) Cadmium (Cd) Lead (Pb) Nickel (Ni)	Direct air-acetylene flame method	Flame Atomic Absorption Spectrophotometer	3111 B. APHA
Mercury (Hg)	Cold Vapour	Atomic Absorption Spectrophotometer	3112. APHA
Arsenic (As)	Continuous Hydride Generation		311C. APHA
Soil samples			
pH	Electrometric	pH meter	Kueneman et al. (2020)
Moisture	Oven drying at 105°C	Oven	
Soil texture	Hydrometer	Hydrometer analysis	
Bulk density	Core sampler	Core sampler	Allison et al. (1954)
Particle density	Pycnometer	Pycnometer	
Organic matter	Loss on Ignition 400°C	Muffle Furnace	
Exchangeable calcium and magnesium	EDTA titrimetric method	Titration	Carter and Gregorich (2007)
Exchangeable potassium	Flame photometry	Flame photometer	
Cation exchange capacity (CEC)	EDTA Titrimetric method	Titration	
Available phosphorus	Olsen method	Spectrophotometer	Motsara and Roy (2008)

2.2.3 Fixed bed column kinetics modelling using YNM, TM, and ABM

The bed saturation of COD in the fixed-bed column was assessed using breakthrough curves (Ghosh et al., 2012; Sugashini and Begum, 2013). This study employed YNM, TM, and ABM to analyse the adsorption kinetics of different soil textures, as these models are widely used and have provided a good fit for column experiments with LL and wastewater (Keerthanan et al., 2021; Nazari, 2017).

YNM assumes that the probability of adsorbate adsorption decreases with time for each molecule (Patel, 2019). The YNM is given by equation (3):

$$\ln\left(\frac{C_t}{C_o - C_t}\right) = (K_{YN} * t) - (K_{YN} * \tau) \quad (3)$$

Where; C_o=influent concentration (mg/L); C_t=outlet concentration at time t (mg/L); K_{YN}=Yoon nelson rate constant (min^{-1}); τ=time required for 50% adsorbate breakthrough.

The adsorption capacity for YNM was determined as a function of M, Co, τ and Q using equation (4):

$$q_{YN} = \frac{\tau C_o Q}{1{,}000M} \quad (4)$$

Where; M=mass of the adsorbent (gm); Co=inlet concentration (mg/L); τ=time required for 50% adsorbate breakthrough (day); Q=flow rate (mL/day).

TM assumes Langmuir kinetics of the adsorption-desorption process to reach equilibrium,

and the maximum adsorption capacity of a bed can be determined using TM (Han et al., 2009). The TM is given by equation (5):

$$\ln\left(\frac{C_o}{C_t}-1\right) = (K_{TH} * Q_o * \frac{M}{Q}) - (K_{TH} * C_o * t) \quad (5)$$

Where; C_o=Influent concentration (mg/L); C_t=outlet concentration at time t (mg/L); K_{TH}=Thomas rate constant (L/mg·day); Q_o=amount adsorbed at equilibrium (mg/g); Q=Flow rate (mL/day); M=mass of adsorbent (g).

ABM is predicated on the idea that the rate of adsorption is determined by the concentration of the sorbing species and the residual adsorption capacity (Patel, 2019). The ABM is given by equation (6):

$$\ln\left(\frac{C_t}{C_o}\right) = K_{AB} * C_o * t - K_{AB} * N_o * \left(\frac{Z}{U_o}\right) \quad (6)$$

Where; C_o=influent concentration (mg/L); C_t=outlet concentration at time t (mg/L); K_{AB}=Adam and Bohart rate constant (L/mg·day); N_o=adsorption capacity of the bed (mg/L); Z=bed depth (cm); U_o=Superficial velocity (cm/day); t=Time (day).

2.2.4 Model performance evaluation and COD attenuation prediction

The experimental COD data from fixed-bed column tests and model-predicted (C_t) values from YNM, TM, and ABM for various soil textures were compared using the coefficient of determination (R^2) and root mean square error (RMSE). Observed concentrations ($y_1 \ldots y_n$) and model values ($f_1 \ldots f_n$) were evaluated, with models showing R^2 near unity and lower RMSE values selected for COD prediction across soil textures. The average of the experimental data is computed by equation (7):

$$\bar{y} = \frac{1}{n}\sum_{i=1}^{n} y_i \quad (7)$$

The total sum of squares SS_{tot} of the data set is given by equation (8):

$$SS_{tot} = \sum_i (y_i - \bar{y})^2 \quad (8)$$

The total squared residuals SS_{res} given by equation (9):

$$SS_{res} = \sum_i (y_i - f_i)^2 \quad (9)$$

Then the coefficient of determination (R^2) is calculated using equation (10):

$$R^2 = 1 - \frac{SS_{res}}{SS_{tot}} \quad (10)$$

The Root means square error (RMSE) is calculated using equation (11):

$$RMSE = \sqrt{\frac{\sum_{i=1}^{n}(y_i - f_i)^2}{n}} \quad (11)$$

Where; n is the number of observations.

3. RESULTS AND DISCUSSION

3.1 Physicochemical and heavy metal characteristics of LL

The physicochemical and heavy metal characteristics of leachate from the Bancharedada landfill site, averaged over 12 months, are summarised in Table 3 and compared with typical young (acetogenic) leachate. As the Bancharedada landfill site is only 2 years old (<5 years), its leachate can be classified as acetogenic (Bashir et al., 2015). The characteristics of young (acetogenic) leachate reported by Wijekoon et al. (2022) indicate pH values ranging from acidic to alkaline (4.5-7.5), and Electrical Conductivity (EC) ranging from 7,000-30,000 µs/cm, which aligns with the findings of the present study. BOD_5 values in this study ranged from 1,240-2,238 mg/L, with an average of 1,816 mg/L, consistent with the 13.1-6,350 mg/L range reported by Scott et al. (2005) for leachate from large landfills. COD values (2,647-4,650) mg/L fall within the 1,500-7,100 mg/L range observed by Scott et al. (2005) but remain lower than the >10,000 mg/L reported by Foo and Hameed (2009).

The BOD_5/COD ratio (0.44-0.50) in this study is comparable to findings by Bashir et al. (2015). Ammoniacal nitrogen (NH_3-N) ranged from 2.86 to 8.59 mg/L, well below the <400 mg/L limit reported by Foo and Hameed (2009). Total Kjeldahl Nitrogen (TKN) values (638-1,174 mg/L) and chloride concentrations (428-1,094 mg/L) fall within typical ranges reported for young leachate by Mukherjee et al. (2015). Heavy metals were in the low to medium range (Adhikari and Khanal, 2015). Specifically, Fe (4.5-17.87 mg/L), Zn (0.2-2.52 mg/L), and Mn (3.32-9.4) mg/L were all within the expected ranges for acetogenic leachate (Scott et al., 2005).

Table 3. Minimum, maximum, average, standard deviation and median of physicochemical and heavy metals characteristics of raw LL from the Bancharedada landfill site

S.no.	Parameters	Unit	Minimum	Maximum	Average±SD	Median
1	pH	-	6.5	7.8	7±0.42	6.9
2	EC	µs/cm	16,230	18,964	18,274.58±869.88	18,770.5
3	TDS	mg/L	3,654	5,664	4,672.50±691.07	4,754.5
4	BOD_5	mg/L	1,240	2,238	1,816.00±342.33	1,956
5	COD	mg/L	2,647	4,650	3,853.33±696.22	3,984.5
6	BOD_5/COD	-	0.44	0.50	0.48±0.02	0.48
7	TKN	mg/L	638	1174	987.50±143.44	985
8	NH_3-N	mg/L	2.86	8.59	5.72±2.18	5.245
9	NO_3-N	mg/L	1.35	4.89	4.05±1.00	4.4
10	Cl	mg/L	428	1,094	945.67±186.45	1,002
11	Fe	mg/L	4.5	17.87	15.75±4.03	17.385
12	Cu	mg/L	0.05	0.4	0.17±0.13	0.105
13	Ni	mg/L	0.1	0.94	0.53±0.26	0.5
14	Zn	mg/L	0.2	2.52	1.38±0.91	1.565
15	Pb	mg/L	0.09	0.36	0.21±0.10	0.21
16	Cr	mg/L	0.05	0.35	0.20±0.09	0.2
17	Hg	mg/L	0.001	0.213	0.02±0.06	0.003
18	As	mg/L	0.011	0.105	0.05±0.03	0.037
19	Cd	mg/L	0.01	0.052	0.04±0.02	0.0435
20	Mn	mg/L	3.32	9.4	6.18±1.66	6.31
21	Total Coliform	CFU/100 mL	170,000	241,500	222,067±220,622	230,825

SD: represents the standard deviation

3.2 Seasonal variations of LL

Seasonal variations in Bancharedada landfill site leachate characteristics (Table 4) reflect Nepal's wet (July-August) and dry (December-February) periods. BOD_5 levels were highest in winter (2,086.67) mg/L and lowest in the post-monsoon (1,475.00 mg/L), as shown in Figure 3. This pattern is likely attributed to increased oxygen availability and reduced biodegradation rates at lower temperatures (Ashraf et al., 2022). COD concentrations peaked during the pre-monsoon (4,499.67 mg/L) and were lowest in the post-monsoon (3,083.00 mg/L). Elevated BOD_5 and COD in dry seasons suggest limited dilution, whereas monsoon rainfall increased the leachate volume and diluted pollutant concentrations (Rhouat et al., 2019; Hoai et al., 2021).

The BOD_5/COD ratio (0.44-0.51) was higher in the dry season and lower during the monsoon, indicating moderate biodegradability and typical characteristic of young leachate (Bernardo-Bricker et al., 2014). Ratios greater than 0.5 are typical of young landfills (<5 years),whereas ratios close to 0.1 are associate with stabilised landfills (>10 years) as reported by Ghahrchi and Rezaee (2020). With an operational age of two years (since May 2022) and a BOD_5/COD ratio between 0.44-0.51, the leachate aligns with the characteristics of a young landfill. Seasonal fluctuations are primarily influenced by climate factors (temperature and precipitation) and site-specific conditions: monsoon rainfall dilutes contaminants, while dry periods yield more concentrated leachate (Al-Yaqout and Hamoda, 2020).

3.3 Seasonal fluctuations of LPI

Seasonal variations in overall LPI and its sub-indices (LPIor, LPIin, and LPIhm) are shown in Table 5. Both LPIor and LPIin were consistently higher than LPIhm, indicating dominance of organic and inorganic pollutants in LL from the Bancharedada landfill site. LPIor was lowest during the monsoon (59.52) and highest in winter (64.09), reflecting the trend of the BOD_5/COD ratio shown in Figure 3. LPIin also varied seasonally, from 10.19 in the monsoon to 13.09 in winter. The overall LPI followed the order: winter > pre-monsoon > post-monsoon > monsoon, suggesting higher pollutant concentrations during the dry seasons.

Table 4. Seasonal variations in physicochemical and heavy metals characteristics of raw leachate from the Bancharedada landfill site

S.no.	Parameters	Unit	Pre-monsoon (average±SD)	Monsoon (average±SD)	Post-monsoon (average±SD)	Winter (average±SD)
1	pH	-	6.70±0.26	7.07±0.64	7.40±0.20	6.83±0.12
2	EC	µs/cm	18,917.33±45.09	17,500.00±1,270.00	17,844.00±518.10	18,837.00±78.63
3	TDS	mg/L	5,366.67±412.30	4,584.00±930.00	3,943.67±169.74	4,795.67±94.16
4	BOD_5	mg/L	2,046.33±133.61	1,657.50±417.50	1,475.00±186.70	2,086.67±183.89
5	COD	mg/L	4,499.67±133.61	3,749.00±901.00	3,083.00±408.16	4,081.67±241.72
6	BOD_5/COD	-	0.46±0.02	0.44±0.01	0.48±0.003	0.51±0.015
7	TKN	mg/L	1,116.00±79.02	895.00±257.00	944.67±9.87	994.33±18.50
8	NH_3-N	mg/L	8.40±0.20	5.61±2.75	3.78±0.13	5.07±1.25
9	NO_3-N	mg/L	4.79±0.14	3.07±1.72	3.89±0.07	4.45±0.14
10	Cl	mg/L	1,063.00±37.03	761.00±333.00	948.00±19.00	1,010.67±20.53
11	Fe	mg/L	17.44±0.25	10.83±6.33	17.29±0.86	17.44±0.10
12	Cu	mg/L	0.07±0.02	0.09±0.03	0.14±0.08	0.36±0.05
13	Ni	mg/L	0.73±0.12	0.49±0.41	0.30±0.18	0.57±0.13
14	Zn	mg/L	2.36±0.20	0.76±0.57	0.41±0.21	1.99±0.35
15	Pb	mg/L	0.31±0.06	0.17±0.10	0.12±0.04	0.25±0.07
16	Cr	mg/L	0.20±0.06	0.10±0.06	0.19±0.08	0.31±0.06
17	Hg	mg/L	0.01±0.01	0.07±0.12	0.004±0.001	0.002±0.001
18	As	mg/L	0.04±0.01	0.04±0.04	0.08±0.05	0.03±0.01
19	Cd	mg/L	0.02±0.01	0.03±0.02	0.05±0.00	0.05±0.00
20	Mn	mg/L	7.07±0.67	6.09±3.08	4.81±0.62	6.74±0.59
21	Total coliform	CFU/100 mL	239,050	205,767	208,950	234,500
Temperature minimum (ºC)			10.39	16.77	12.88	5.20
Temperature maximum (ºC)			21.16	22.74	20.03	14.00
Precipitation (mm)			192.00	1,799.40	496.00	17.00

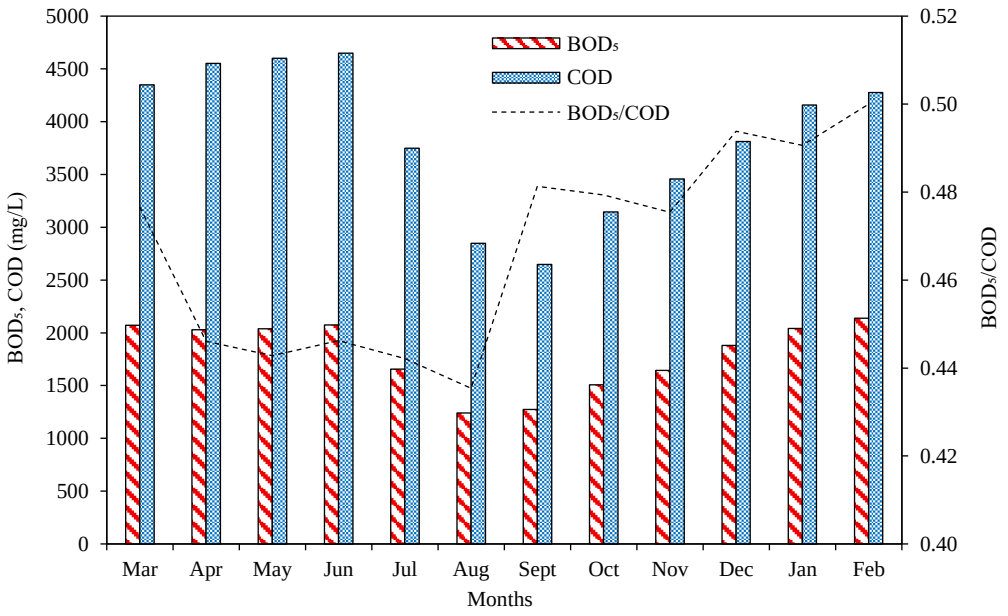

Figure 3. Seasonal variation of BOD_5, COD, and BOD_5/COD ratio of leachate from Bancharedada landfill site

Table 5. Seasonal fluctuations of Overall LPI, LPI_{or}, LPI_{in}, and LPI_{hm}

Pre-monsoon							Monsoon					Post-monsoon					Winter				
Index	Parameter	Value	Pi	Wi	WiPi	LPI	Value	Pi	Wi	WiPi	LPI	Value	Pi	Wi	WiPi	LPI	Value	Pi	Wi	WiPi	LPI
LPI_{or}	BOD_5	2,046	35	0.263	9.21	63.16	1,706	30	0.267	8.01	59.52	1,475	30	0.267	8.01	59.52	2,086	40	0.267	9.345	64.09
	COD	4,500	60	0.267	16.02		3,749	55	0.263	14.465		3,083	55	0.263	14.47		4,082	62	0.263	15.78	
	Coliform	239,050	100	0.224	22.4		205,767	100	0.224	22.4		208,950	100	0.224	22.4		234,500	100	0.224	22.4	
LPI_{in}	pH	6.7	5	0.214	1.07	13.09	7.07	5	0.214	1.07	10.19	7.4	5	0.214	1.07	11.05	6.83	5	0.214	1.07	13.09
	NH_3-N	8.4	5	0.198	0.99		5.61	5	0.198	0.99		3.78	5	0.198	0.99		5.07	5	0.198	0.99	
	Cl	1,063	10	0.187	1.87		761	5.5	0.187	1.0285		948	9.8	0.187	1.833		1,010.67	10	0.187	1.87	
	TDS	5,367	10	0.195	1.95		4,584	10	0.195	1.95		3,944	5	0.195	0.975		4,796	10	0.195	1.95	
	TKN	1,116	35	0.206	7.21		895	25	0.206	5.15		944.67	30	0.206	6.18		994.33	35	0.206	7.21	
LPI_{hm}	Fe	17.44	5	0.088	0.44	5.00	10.83	5	0.088	0.44	5.00	17.293	5	0.088	0.44	5.00	17.443	5	0.088	0.44	5.00
	Cu	0.07	5	0.098	0.49		0.09	5	0.098	0.49		0.1433	5	0.098	0.49		0.360	5	0.098	0.49	
	Ni	0.73	5	0.102	0.51		0.49	5	0.102	0.51		0.3	5	0.102	0.51		0.573	5	0.102	0.51	
	Zn	2.36	5	0.11	0.55		0.76	5	0.11	0.55		0.41	5	0.11	0.55		1.987	5	0.11	0.55	
	Pb	0.31	5	0.123	0.615		0.17	5	0.123	0.615		0.1233	5	0.123	0.615		0.247	5	0.123	0.615	
	Cr	0.2	5	0.125	0.625		0.10	5	0.125	0.625		0.1933	5	0.125	0.625		0.313	5	0.125	0.625	
	As	0.04	5	0.137	0.685		0.04	5	0.137	0.685		0.0777	5	0.137	0.685		0.035	5	0.137	0.685	
	Hg	0.01	5	0.121	0.605		0.073	5	0.121	0.605		0.004	5	0.121	0.605		0.002	5	0.121	0.605	
Overall LPI						20.57					18.98					19.20					20.79

3.4 Physicochemical characteristics of soil samples

The physicochemical characteristics of soil samples used in the fixed-bed column tests are summarised in Table 6. Based on the United States Department of Agriculture (USDA) classification, the soils represent seven textures: S1—clayey, S2—silt loam, S3—sandy, S4—loam, S5—sandy loam, S6—clay loam, and S7—silt loam. The characteristics observed across these samples, ranging from clay-rich to sandy textures, demonstrate substantial natural variability consistent with Nepal's heterogeneous soil environment. Sand, silt, and clay content varied widely (12.68-88%, 9-60%, and 3-56%, respectively), with corresponding differences in porosity (31-48%) and cation exchange capacity (CEC) (7.63-11.68 cmol/kg). These variations align with the diverse soil types reported across Nepal's physiographic regions, which are shaped by pronounced altitudinal gradients and differences in parent material (Nepal et al., 2023). Fine-textured soils (clayey, silt loam and clay loam) exhibited higher moisture content, organic matter, and CEC values consistent with those found in Nepal's Terai and hill regions (Shrestha et al., 2017).

Table 6. Physicochemical characteristics of soil samples

Parameters	Unit	S1	S2	S3	S4	S5	S6	S7
Moisture content	%	7.92	8.3	4.52	6.95	3.46	5.68	4.16
pH	-	6.3	5.9	6.2	7.3	6.6	6.65	6.22
Soil texture	Sand (%)	12.68	14.00	88.00	37.65	63.99	25.92	32.88
	Silt (%)	31.32	60.00	9.00	46.34	21.00	46.07	59.11
	Clay (%)	56.00	26.00	3.00	16	15.00	28.00	8.00
USDA classification of soil textures		Clayey	Silt loam	Sandy	Loam	Sandy loam	Clay loam	Silt loam
Bulk density	g/cm^3	1.35	1.42	1.65	1.5	1.45	1.45	1.33
Particle density	g/cm^3	2.32	2.42	2.45	2.32	2.28	2.52	2.38
Porosity	%	31	37	48	42	36	42	38
Organic matter	%	7.62	7.40	2.53	4.46	0.53	5.86	6.88
Carbon	%	4.28	2.48	0.5	2.58	0.3	3.4	3.99
Total nitrogen	%	0.38	1.26	1.12	1.67	1.96	1.21	2.69
Phosphorus	mg/kg	4.42	2.48	1.56	2.896	3.84	1.496	2.304
Potassium	mg/kg	1,243	1,037	1,068	1,444	1,245	1,156	1,356
Calcium	mg/kg	518	487	309	319	348	412	559
Magnesium	mg/kg	253	143	98	168	102	118	327
CEC	cmol/kg	11.68	8.02	7.89	7.95	7.63	10.81	9.17

3.5 Breakthrough curve analysis for different soil textures

The breakthrough curves for S1-S7 soil samples, classified per USDA soil textures are presented in Figure 4. The results show that lower soil porosity shortens the bed saturation time by reducing the contact time between adsorbate molecules and adsorbent pore surfaces. During the first 12 h, no filtrate was observed for S1, S2, S3, S4, S5, S6, and S7 whereas S3 (sandy) exhibited a breakthrough at 1 h. Bed saturation times were 35, 22, 4, 15, 11, 18, and 12 days for S1-S7 soils, respectively. The shape of the breakthrough curve is affected by the porosity and clay percentage of soils. Lower porosity and clay percentages result in longer contact times due to reduced hydraulic conductivity, allowing the absorbate molecules more time to diffuse into the adsorbent's pores and thereby increasing the bed's adsorption efficiency (Foo, 2020; Yahya et al., 2021). Clayey soil (31% porosity) reached 99% influent concentration of day 35, whereas sandy soil (48% porosity) reached saturation by day 4. Consequently, fine-textured soils with higher organic matter and CEC offer greater potential for COD adsorption and microbial activity, while sandy soils exhibit faster leachate breakthrough and reduced attenuation (Koirala et al., 2019). These findings suggest that leachate attenuation capacity in Nepal cannot be generalized; rather, it is strongly influenced by the combined effects of soil texture, mineralogy, and seasonal rainfall patterns.

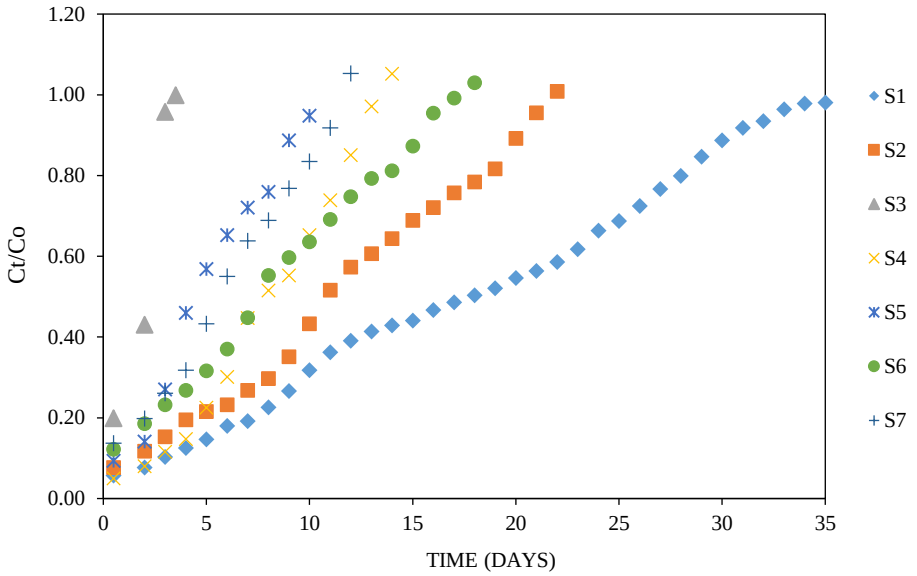

Figure 4. Breakthrough curves from column tests done in S1-S7 soil samples with LL for COD

3.6 Column kinetics for COD adsorption using three models

3.6.1 YNM, TM, and ABM models

The parameters obtained from fitting experimental data with YNM, TM, and ABM are shown in Table 7. Plotting $\ln(\frac{C_t}{C_o - C_t})$ against time yielded the YN rate constant K_{YN} of 0.16, 0.23, 2.39, 0.42, 0.52, 0.31, and 0.39 L/day, with corresponding τ (50% adsorbate breakthrough) values of 16.76, 11.06, 1.56, 7.84, 4.90, 7.43, and 5.66 days for S1, S2, S3, S4, S5, S6, and S7 soil samples, respectively. The corresponding adsorption capacities (q_{YN}) were 22.77, 14.82, 1.92, 10.76, 6.59, 10.24, and 7.72 mg/g, respectively.

Plotting $\ln(\frac{C_o}{C_t} - 1)$ against time yielded the TM rate constant K_{th} of 0.6, 0.9, 3.8, 1.6, 2.0, 1.2 and 1.5 (L/mg·day)*10^-4, and the adsorption capacities (Q_o) of 22.78, 14.82, 2.42, 10.76, 6.59, and 10.24 mg/g for S1, S2, S3, S4, S5, S6, and S7 soil samples, respectively.

Plotting $\ln(\frac{C_t}{C_o})$ against time yielded ABM rate constants K_{AB} of 0.3, 0.4, 2.1, 0.8, 0.9, 0.4, and 0.7 (L/mg·day)*10^-4 and adsorption capacity N_o values of 41,957, 26,934, 4,575, 17,222, 12,417, 21,447, and 14,700 mg/L for S1, S2, S3, S4, S5, S6, and S7 soil samples, respectively.

The model parameters showed that soils with higher clay content have lower adsorption rate constants and substantially higher adsorption capacities. S1 (clayey, 56%) showed lower adsorption rate constants with greater adsorption capacity, whereas S3 (sandy, 3% clay) exhibited the opposite trend. The high surface charge and low hydraulic conductivity of clay minerals enhance contaminant removal via ion exchange and adsorption (Foo, 2020), while their strong affinity for contaminants delays rather than removes the pollutants (Khan et al., 2023). Further, in the adsorption mechanism of LL treatment, molecularly imprinted polymers have shown significantly higher adsorption capacity (42.55 mg/g) compared to 7 mg/g for a non-imprinted polymer, demonstrating nearly a sixfold improvement in dye removal from wastewater (Khan et al., 2024). Mxenes-based materials also exhibit strong adsorption performance for heavy metals due to their high surface area and metal ion trapping ability (Zahoor et al., 2024).

The results indicate that clay-rich soils are suitable for landfill cover materials because of their high adsorption capacity and retention of organic pollutants, thereby protecting underlying soils and groundwater. Better adsorption in clay covers decreases the concentration of contaminants entering the leachate collection system, which lowers the operational load on leachate treatment facilities and reduces long-term costs.

Table 7. Obtained parameters from fitting the experimental data with YNM, TM, and ABM for the adsorption of COD in different soil textures

Soil textures	(Co) mg/L	Mass (gm)	YNM				TM			ABM		
			K_{YN} (L/day)	τ (days)	q_{YN} (mg/g)	R^2	K_{th} (L/mg·day)*10^-4	Q_o (mg/g)	R^2	K_{AB} (L/mg·day)*10^-4	N_o (mg/L)	R^2
S1	2,647	487	0.16	16.76	22.77	0.95	0.6	22.78	0.95	0.3	41,957	0.89
S2	2,647	494	0.23	11.06	14.82	0.96	0.9	14.82	0.96	0.4	26,934	0.94
S3	2,647	537	1.01	1.98	2.44	0.90	3.8	2.42	0.90	2.1	4,575	0.97
S4	2,647	482	0.42	7.84	10.76	0.96	1.6	10.76	0.96	0.8	17,222	0.94
S5	2,647	492	0.52	4.90	6.59	0.98	2.0	6.59	0.98	0.9	12,417	0.88
S6	2,647	480	0.31	7.43	10.24	0.92	1.2	10.24	0.92	0.4	21,447	0.93
S7	2,647	485	0.39	5.66	7.72	0.99	1.5	7.73	0.99	0.7	14,700	0.96

Table 8. SS_{tot}, SS_{res}, R^2, and RMSE obtained from model evaluation

Soil textures	YNM				TM				ABM			
	SS_{tot} (*10^6)	SS_{res} (*10^5)	R^2	RMSE	SS_{tot} (*10^6)	SS_{res} (*10^5)	R^2	RMSE	SS_{tot} (*10^6)	SS_{res} (*10^5)	R^2	RMSE
S1	39	16	0.959	151.88	39	806	-1.07	1,073.55	39	68	0.825	312.11
S2	24	2	0.989	78.95	24	517	-1.08	1,083.98	24	35	0.858	283.08
S3	557	6	0.999	307.06	557	60	0.70	931.96	557	2	0.988	189.86
S4	22	6	0.972	147.01	22	460	-1.09	1,260.20	22	41	0.942	376.87
S5	13	2	0.983	102.85	13	211	0.65	1,002.48	13	36	0.940	414.17
S6	19	4	0.978	109.18	19	304	-0.53	919.40	19	25	0.976	264.13
S7	13	2	0.981	103.32	13	218	-0.60	954.50	13	12	0.981	226.08

3.7 Model evaluation and prediction

Three models (YNM, TM, and ABM) were evaluated for predicting COD concentrations in leachate through soil columns. Table 8 compares their performance using the total sum of squares (SS_{tot}), residual sum of squares (SS_{res}), coefficient of determination (R^2), and RMSE. A higher R^2 value (closer to 1) indicates better predictive accuracy and reliability (Yousefi Kebria et al., 2018; Patel, 2019).

The R^2 and RMSE values across different soil textures indicate that YNM and ABM better predict COD concentrations than TM, with YNM performing the best due to consistently higher R^2 (closer to 1) and lower RMSE. The TM produced negative R^2 values across most soil textures, indicating that its residual variance exceeded the total variance, which means this model demonstrates poor predictive capability for the adsorption breakthrough behaviour in all soil textures. Therefore, Figure 5 shows the fit between observed COD values and those predicted by YNM. Similar findings were reported by Kovo et al. (2023), where YNM effectively predicted COD in a column study using magnetite-zeolite composites. Zhang et al. (2022) also found YNM to be reliable in modelling Cr (VI) adsorption in red mud leachate onto clay layers.

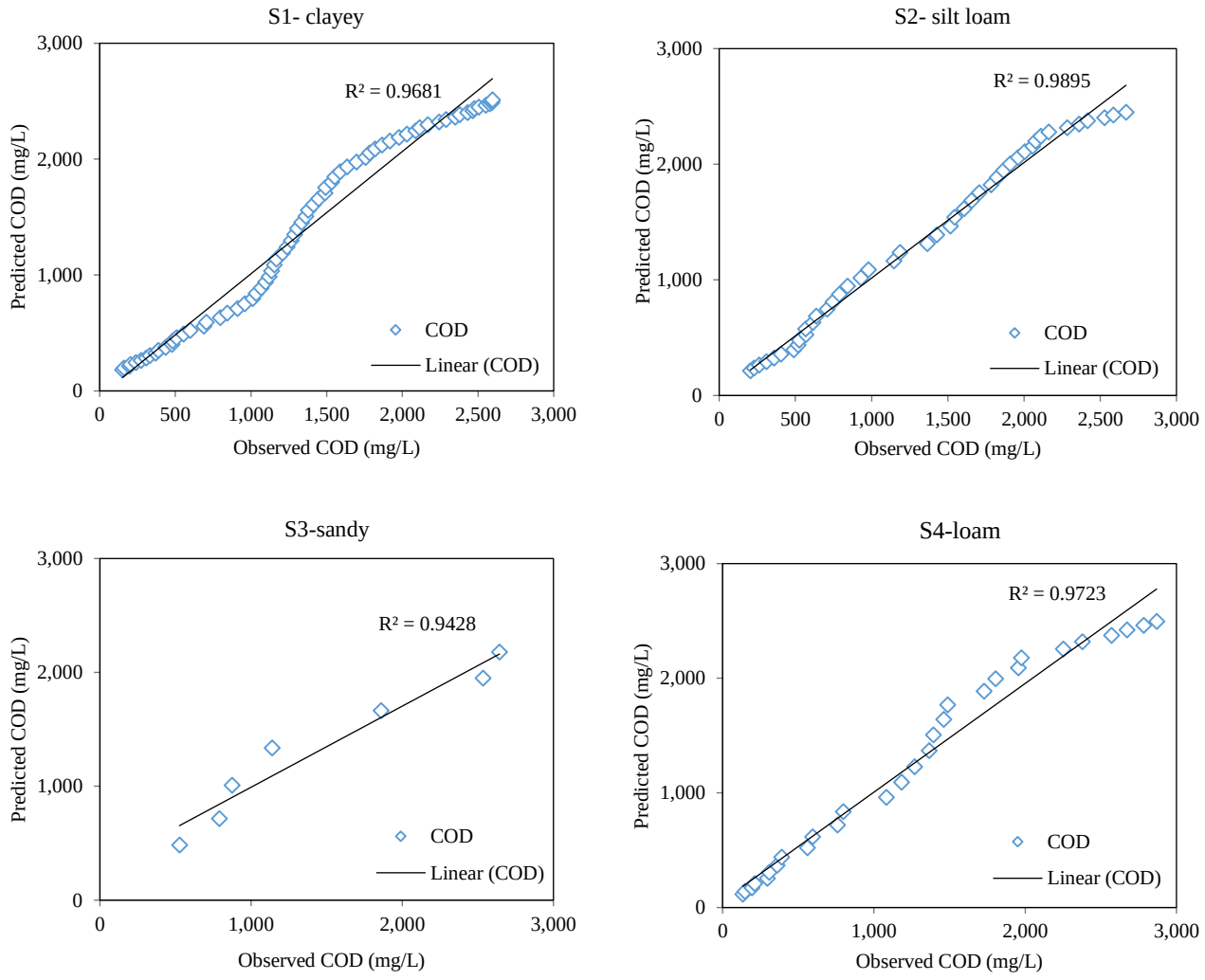

Figure 5. Regression line for all of the S1-S7 soil textures of the for observed and predicted values using YNM

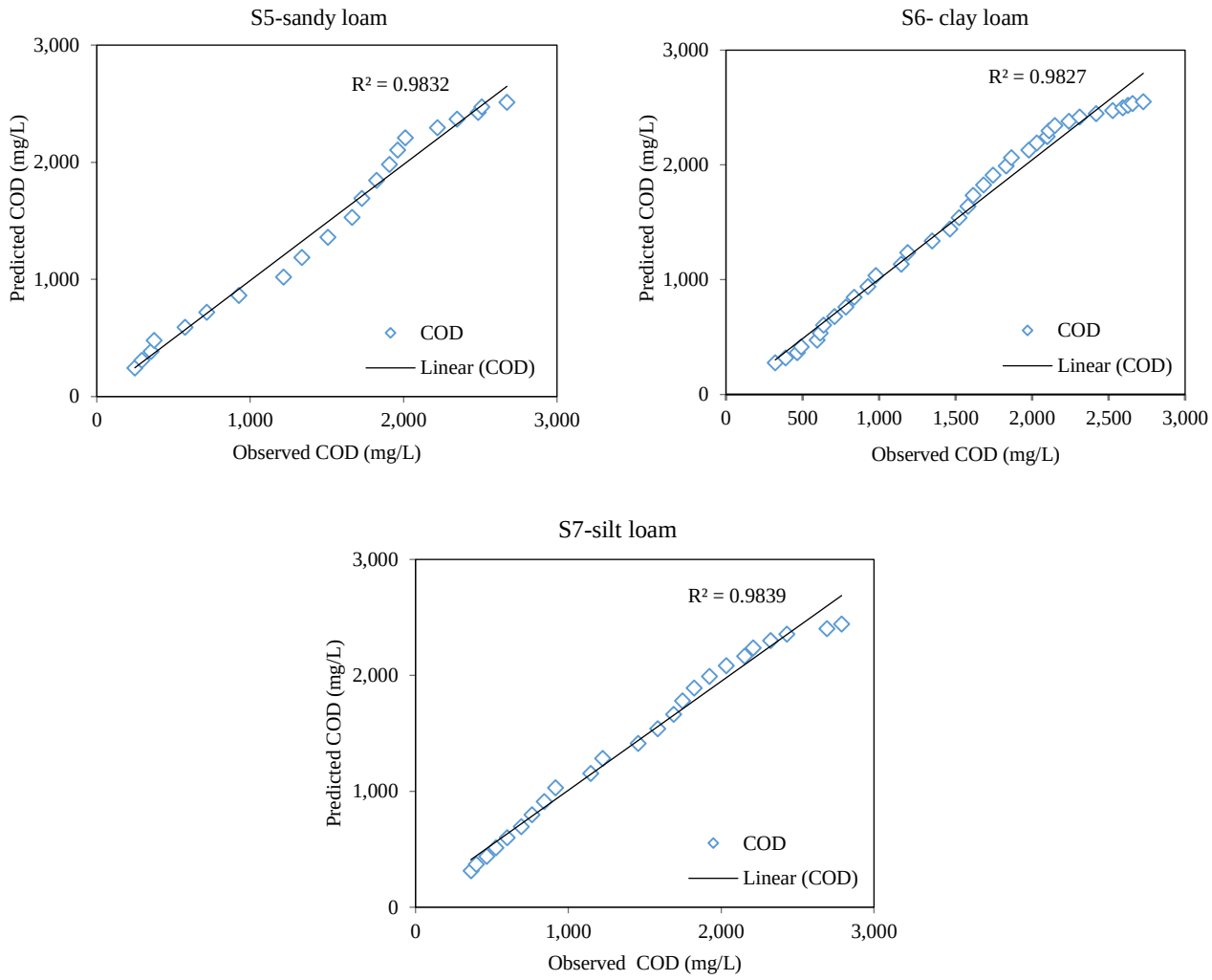

Figure 5. Regression line for all of the S1-S7 soil textures of the observed and predicted values using YNM (cont.)

4. CONCLUSION

Seasonal LPI fluctuations indicated that organic content significantly influences leachate pollution at the Bancharedada landfill site. Experimental results showed that clay-rich soils effectively delay the transport of organic contaminants, highlighting their suitability as landfill cover materials in landfill design. Among the three kinetic models (YNM, TM, and ABM) tested, YNM achieved the highest predictive accuracy (lowest RMSE), followed by ABM, which also performed acceptably based on RMSE and R^2 metrics. YNM parameters (K_{YN}) showed strong correlations with soil texture, confirming its reliability for predicting COD attenuation. Future studies should examine soils with higher clay fractions and consider factors such as adsorbent dosage, loading rate, and contact time for on-site leachate remediation. Additional experiments incorporating locally available amendments such as biochar or compost would also help assess their potential to enhance soil sorption capacity for other pollutants.

ACKNOWLEDGEMENTS

The authors would like to acknowledge the Soil, Water, and Air Testing Laboratories Pvt. Ltd. for the technical support and space for the experimental works. No authors received any funding or financial support for this research.

AUTHOR CONTRIBUTIONS

Conceptualisation, Methodology, Investigation, Formal Analysis, Visualisation, Validation, and Writing-original draft, Lokesh Sapkota; Investigation, Sophie Shrees and Aalekh Bhattarai; Supervision, Rajendra Joshi, Anish Ghimire, Bikash Adhikari; Writing-review and editing, Anish Ghimire, Rajendra Joshi, Bikash Adhikari, Bijay Thapa.

DECLARATION OF CONFLICT OF INTEREST

Dr. Anish Ghimire serves as a member of the editorial board for the Environment and Natural Resources Journal. He has not participated in any peer review processes. The authors declare that there are no competing interests.

REFERENCES

Adhikari B, Khanal SN. Qualitative study of landfill leachate from different ages of landfill sites of various countries including Nepal. IOSR Journal of Environmental Science, Toxicology and Food Technology 2015;9:23-36.

Al-Yaqout A, Hamoda MF. Long-term temporal variations in characteristics of leachates from a closed landfill in an arid region. Water, Air, and Soil Pollution 2020;231:Article No. 319.

Allison L, Bernstein L, Bower CA, Brown JW, Fireman M, Hatcher JT, et al. Diagnosis and Improvement of Saline and Alkaline Soils. Vol. 18. Washington, DC: United States Department of Agriculture; 1954.

Ashraf M, Zeshan M, Hafeez S, Hussain R, Qadir A, Majid M, et al. Temporal variation in leachate composition of a newly constructed landfill site in Lahore in context to environmental pollution and risks. Environmental Science and Pollution Research 2022;29:37129-43.

Baird RB, Eaton AD, Rice EW. Standard Methods for the Examination of Water and Wastewater, American Public Health Association. 23rd ed. Washington, DC: American Public Health Association, American Water Works Association, Water Environment Federation; 2017.

Bashir MJK, Aziz HA, Amr SSA, Sethupathi S, Ng CA, Lim JW. The competency of various applied strategies in treating tropical municipal landfill leachate. Desalination and Water Treatment 2015;54:2382-95.

Bernardo-Bricker AR, Singh SK, Trovó AG, Tang WZ, Tachiev G. Biodegradability enhancement of mature landfill leachate using fenton process under different COD loading factors. Environmental Processes 2014;1:207-19.

Carter MR, Gregorich EG. Soil Sampling and Methods of Analysis. Ottawa: Canadian Society of Soil Science; 2007.

Central Bureau of Statistics. Waste Management Baseline Survey of Nepal 2020. Kathmandu: National Planning Commission, Government of Nepal; 2020.

Chetri JK, Reddy KR. Advancements in municipal solid waste landfill cover system: A review. Journal of the Indian Institute of Science 2021;101:557-88.

Cronan CS. Ecosystem Biogeochemistry. Textbooks in Earth Sciences, Geography and Environment. Springer International Publishing; 2018, p. 11-29.

Foo KY. Potential of natural clay derived functionalized adsorbent for the effective remediation of sanitary landfill leachate. Desalination and Water Treatment 2020;175:164-73.

Foo KY, Hameed BH. An overview of landfill leachate treatment via activated carbon adsorption process. Journal of Hazardous Materials 2009;171:54-60.

Ghahrchi M, Rezaee A. Electro-catalytic ozonation for improving the biodegradability of mature landfill leachate. Journal of Environmental Management 2020;254:Article No. 109811.

Ghosh S, Kumar S, Mukherjee S, Tarafder DD, Hettiaratchi P. Adsorptive chromium removal by some clayey soil for abatement of tannery waste pollution. Journal of Hazardous, Toxic, and Radioactive Waste 2012;16:243-9.

Gonçalves F, Correa CZ, Lopes DD, Vendrame PRS, Teixeira RS. Monitoring of the process of waste landfill leachate diffusion in clay and sandy soil. Environmental Monitoring and Assessment 2019;191:Article No. 577.

Goyal H, Parby JI, Lypiridis C, Lal MK, Soni P, Mondal P, et al. Strategic Assessment of Solid Waste Management Services and Systems in Nepal : City-Level Assessment and Draft Service Improvement Plan for Solid Waste Management For Pokhara Metropolitan City. Washington, DC: World Bank; 2020.

Han R, Wang Yu, Zhao X, Yuanfeng W, Xie F, Cheng J, et al. Adsorption of methylene blue by phoenix tree leaf powder in a fixed-bed column: Experiments and prediction of breakthrough curves. Desalination 2009;245:284-97.

Hoai ST, Lan HN, Viet NTT, Hoang GN, Kawamoto K. Characterizing seasonal variation in landfill leachate using leachate pollution index (LPI) at nam son solid waste landfill in Hanoi, Vietnam. Environments 2021;8(3):Article No. 17.

Hussein M, Yoneda K, Zaki ZM, Othman NA, Amir A. Leachate characterizations and pollution indices of active and closed unlined landfills in Malaysia. Environmental Nanotechnology, Monitoring and Management 2019;12:Article No. 100232.

Kaza S, Lisa Y, Bhada TP, Frank VW. What a Waste 2.0, A Global Snapshot of Solid Waste Management to 2050. Washington, DC: World Bank; 2018.

Keerthanan S, Gunawardane C, Somasundaram T, Jayampathi T, Jayasinghe C, Vithanage M. Immobilization and retention of caffeine in soil amended with Ulva reticulata biochar. Journal of Environmental Management 2021;281:Article No. 111852.

Khan M, Ahmad I, Khan S, Zeb A, Elsadek MF, Patel S. Molecularly imprinted polymer for the selective removal of direct violet 51 from wastewater: synthesis, characterization, and environmental applications. Journal of Polymer Engineering 2024;44(10):761-75.

Khan S, Ajmal S, Hussain T, Rahman MU. Clay-based materials for enhanced water treatment: Adsorption mechanisms, challenges, and future directions. Journal of Umm Al-Qura University for Applied Sciences 2023;11:219-34.

Khanal A. Forecasting municipal solid waste generation using linear regression analysis: A case of Kathmandu Metropolitan City, Nepal. Multidisciplinary Science Journal 2023;5(2): Article No. 19.

Koirala P, Thakuri S, Joshi S, Chauhan R. Estimation of soil erosion in Nepal using a RUSLE modeling and geospatial tool. Geosciences 2019;9:Article No. 147.

Kovo AS, Alaya-Ibrahim S, Abdulkareem AS, Adeniyi OD, Egbosiuba TC, Tijani JO, et al. Column adsorption of biological oxygen demand, chemical oxygen demand and total organic carbon from wastewater by magnetite nanoparticles-zeolite A composite. Heliyon 2023;9:e13095.

Kueneman E, Hopmans JW, Raser E, Martin CCGS, Fisher J. Water-Smart Agriculture A Biophysical Focused Introduction: Addressing Needs and Opportunities in Developing Nations. San José: Inter-American Institute for Cooperation on Agriculture; 2020.

Kumar D, Alappat BJ. Evaluating leachate contamination potential of landfill sites using leachate pollution index. Clean Technologies and Environmental Policy 2005;7:190-7.

Lothe AG, Sinha A. Development of model for prediction of Leachate Pollution Index (LPI) in absence of leachate parameters. Waste Management 2017;63:327-36.

Motsara MR, Roy RN. Guide to Laboratory Establishment for Plant Nutrient Analysis. Rome: Food and Agriculture Organization of the United Nations (FAO); 2008.

Mukherjee S, Mukhopadhyay S, Hashim MA, Gupta BS. Contemporary environmental issues of landfill leachate: Assessment and remedies. Critical Reviews in Environmental Science and Technology 2015;45:472-590.

Naka A, Yasutaka T, Sakanakura H, Kalbe U, Watanabe Y, Inoba S, et al. Column percolation test for contaminated soils: Key factors for standardization. Journal of Hazardous Materials 2016;320:326-40.

Nawaz T, Rahman A, Pan S, Dixon K, Petri B, Selvaratnam T. A review of landfill leachate treatment by microalgae: Current status and future directions. Processes 2020;8:Article No. 384.

Nayanthika IVK, Jayawardana DT, Bandara NJGJ, Manage PM, Madushanka RMTD. Effective use of iron-aluminum rich laterite based soil mixture for treatment of landfill leachate. Waste Management 2018;74:347-61.

Nazari M. The Use of Brown Coal for the Removal of Nutrients from Wastewater [dissertation]. Melbourne, RMIT University, 2017.

Nepal S, K.C. M, Pudasainia N, Adhikari H. Divergent Effects of Topography on Soil Properties and Above-Ground Biomass in Nepal's Mid-Hill Forests. Resources 2023;12:Article No. 136.

Organisation for Economic Co-operation and Development (OECD). OECD Guidelines for the Testing of Chemicals, Section 3. Paris: OECD Publishing; 2004.

Patel H. Fixed-bed column adsorption study: A comprehensive review. Applied Water Science 2019;9:Article No. 45.

Pathak DR, Mainali B, Abuel-Naga H, Angove M, Kong I. Quantification and characterization of the municipal solid waste for sustainable waste management in newly formed municipalities of Nepal. Waste Management and Research 2020;38:1007-18.

Qi G, Yue D, Liu J, Li R, Shi X, He L, et al. Impact assessment of intermediate soil cover on landfill stabilization by characterizing landfilled municipal solid waste. Journal of Environmental Management 2013;128:259-65.

Regadío M, Ruiz AI, Rodríguez-Rastrero M, Cuevas J. Containment and attenuating layers: An affordable strategy that preserves soil and water from landfill pollution. Waste Management 2015;46:408-19.

Rhouat S, El Youbi MS, Dimane F. Physico-chemical characterization of Meknes municipal landfill leachate and assessment of the seasonal effects using PCA. Environmental Engineering and Management Journal 2019;18:2405-15.

Scott J, Beydoun D, Amal R, Low G, Cattle J. Landfill management, leachate generation, and leach testing of solid wastes in Australia and overseas. Critical Reviews in Environmental Science and Technology 2005;35:239-332.

Shrestha HL, Bhandari TS, Karky BS, Kotru R. Linking soil properties to climate change mitigation and food security in Nepal. Environments 2017;4:Article No. 29.

Sugashini S, Begum KMMS. Performance of ozone treated rice husk carbon (OTRHC) for continuous adsorption of Cr (VI) ions from synthetic effluent. Journal of Environmental Chemical Engineering 2013;1:79-85.

Teng C, Zhou K, Peng C, Chen W. Characterization and treatment of landfill leachate: A review. Water Research 2021;203:Article No. 117525.

Wijekoon P, Koliyabandara PA, Cooray AT, Lam SS, Athapattu BCL, Vithanage M. Progress and prospects in mitigation of landfill leachate pollution: Risk, pollution potential, treatment and challenges. Journal of Hazardous Materials 2022;421:Article No. 126627.

Yahya MD, Imam IA, Abdulkareem SA. Column adsorption studies for the removal of chemical oxygen demand from fish pond wastewater using waste alum sludge. In: Advances in Remediation Techniques for Polluted Soils and Groundwater. Elsevier; 2021. p. 21-48.

Yidong G, Xin C, Shuai Z, Ancheng L. Performance of multi-soil-layering system (MSL) treating leachate from rural unsanitary landfills. Science of the Total Environment 2012;420:183-90.

Yousefi Kebria D, Ghavami M, Javadi S, Goharimanesh M. Combining an experimental study and ANFIS modeling to predict landfill leachate transport in underlying soil: A case study in north of Iran. Environmental Monitoring and Assessment 2018;190:Article No. 26.

Zahoor M, Ikram M, Khan S, Ali S. Mxene a versatile hybrid inorganic nanomaterial: A useful adsorbent for the removal of toxic heavy metals and its other applications. Inorganic Chemistry Communications 2024;170:Article No. 113157.

Zhang Y, Yu Y, Qin H, Peng D, Chen X. Dynamic adsorption characteristics of Cr (VI) in red-mud leachate onto a red clay anti-seepage layer. Toxics 2022;10:Article No. 606.